

ACTIVE SOUND TRANSMISSION CONTROL OF AN EXPERIMENTAL DOUBLE-PANEL PARTITION USING DECOUPLED ANALOG FEEDBACK CONTROL

Jason Sagers

Mechanical Engineering, Brigham Young University
Provo, UT 84602

ABSTRACT

This paper addresses the construction, measurement, and analysis of a double panel active partition (DPAP) and its accompanying analog feedback controllers. The DPAP was constructed by attaching an aluminum cone loudspeaker at each end of a short segment of a circular duct. Two analog feedback controllers were designed and built using the measured frequency response function of each panel. Two independent (decoupled) feedback controllers were then used to minimize the vibration amplitude of each panel in the presence of an acoustic disturbance. A normal-incidence transmission loss measurement system was used to assess the performance of the DPAP and of a single panel passive partition. Error signal attenuations show that it is both feasible and effective to simultaneously control both panels with decoupled feedback controllers, and that simultaneously controlling both panels of the DPAP has a distinct advantage over controlling a single panel. The reduction in vibration amplitude across the surface of the transmitting panel was confirmed with scanning laser vibrometer measurements. Transmission loss results were obtained for two passive and three active configurations. The average normal incidence transmission loss over the active measurement bandwidth (50-1,000 Hz) for the active double panel was 60 dB. This is an average of 39 dB more transmission loss than a passive single panel partition.

INTRODUCTION

There has long been interest in the use of partitions to reduce sound transmission into noise-sensitive environments. There is particular need for the improvement of partitions at frequencies where the passive transmission loss is inadequate. This is the case in single and double panel partitions where the transmission loss is severely degraded at low frequencies due to resonance effects. The primary passive method to reduce low frequency sound transmission is to add mass to the partition. However, this solution is not feasible for situations where extra weight cannot be tolerated, such as in aerospace vehicles, large ceiling structures, high rise buildings, etc. A solution to this problem is active structural control.

Active control strategies have been utilized to improve low frequency sound transmission performance. Active structural acoustic control (ASAC) methods have been explored thoroughly [1-12]. This approach involves actuating a continuous transmitting panel in such a way as to minimize the acoustic radiation into the receiving space. ASAC is typically implemented by distributed sensor and actuator pairs that change the radiating mode shapes of the panel in order to

reduce the radiated acoustic power. In general, receiving side attenuations with ASAC methods have been small. Additionally, comparing the performance of one ASAC implementation to another is difficult because the measurement techniques have been inconsistent. Finally, the major drawbacks to the ASAC approach are the large number of fully-coupled actuator/sensor pairs, the need for microphones in the receiving space, and the spatial control spillover that inevitably results when using a continuous transmitting panel.

Effective active sound transmission control (ASTC) has been implemented by Leishman [13-16] wherein the partition is broken into an array of discrete modules that are acoustically and mechanically segmented. The active segmented partition (ASP) allows for localized control of each module, thus eliminating the impracticality of a large number of fully-coupled actuator/sensor pairs that exists for ASAC control. Furthermore, the ASTC approach integrates the error signal sensors inside the cavity of the double panel partition and does not require the placement of microphones in the receiving space. Using digital feed forward active noise control, Leishman achieved single frequency transmission loss results near 60 dB over a band of 30-290 Hz for an array of 4 modules [16]. The primary limitations of Leishman's configuration were its unidirectional performance, need for an advanced reference signal, and lack of broadband control capabilities.

A practical ASTC partition should be bidirectional, stopping sound transmission in both directions through the partition. It is proposed that direct, decoupled actuation of a two panel system might lend itself to bidirectional control. One concern with this actuation scheme is that a fully-coupled MIMO controller would be necessary to counteract the strong acoustic coupling associated with the cavity mode between the two panels. A practical ASTC partition should also be able to control both tonal and broadband noise. An analog feedback controller should more effectively attenuate broadband noise than a digital feed forward scheme.

The purpose of this paper is to explore the performance of analog feedback controllers and panel control on an experimental DPAP module. Furthermore, it will be shown experimentally that effective control can be implemented with two decoupled controllers.

DESIGN OF A TRANSMISSION LOSS MODULE

Module hardware

A prototype double panel active partition (DPAP) module was constructed by using two aluminum cone loudspeakers housed in machined aluminum couplers. The couplers were joined by a 4 inch diameter PVC connecting tube. The cone of each loudspeaker faced outward, towards the source and receiving spaces, and a PCB 352C68 accelerometer was mounted to the center of each speaker cone. A cut away diagram of the DPAP is shown in Figure 1. A cylindrical piece of fiberglass insulation (not shown in the figure) was placed inside the pipe to provide additional passive attenuation at high frequencies and to reduce the strength of the axial cavity resonances.

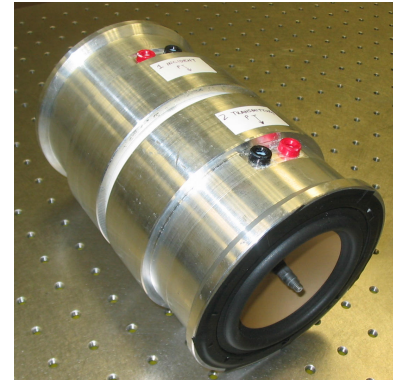


FIGURE 2. ACTUAL DPAP MODULE.

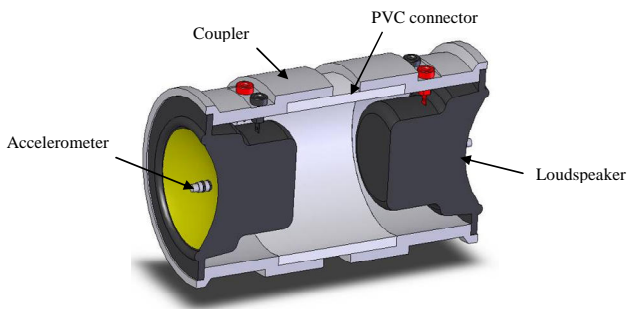


FIGURE 1. CUTAWAY DIAGRAM OF THE DPAP MODULE.

This double panel module was designed with a plane of symmetry to produce bidirectional control capabilities. Each half of the module constitutes a plant, defined as the transfer function between the loudspeaker input and the accelerometer output. Collocated sensor and actuator pairs were used to eliminate phase delay in the plant due to acoustic propagation. This is important to the efficacy of an analog feedback controller.

The ends of the PVC connecting tube were treated with adhesive foam rubber to provide resilient end connections. These resilient connections were necessary to prevent a direct mechanical vibration path through the module, which would compromise the transmission loss measurement. Furthermore, the design ensured that any air gaps into and out of the module were eliminated. For instance, the electrical connections to the loudspeakers were made through airtight banana plug receptacles mounted on the outside of the coupler. A picture of the actual module hardware is shown in Figure 2. The cone to cone length between the speakers was roughly 6 inches. When needed during experimentation, one of the loudspeakers was removed from its housing to create a single-panel partition. The absorptive fill was also removed for this configuration.

Feedback control principles

A block diagram for a generic positive-feedback control scheme is shown in Figure 3. $D(t)$ is a disturbance input (the noise to be cancelled) and $e(t)$ is the error signal. The controller is designated by C and the plant is designated by P .

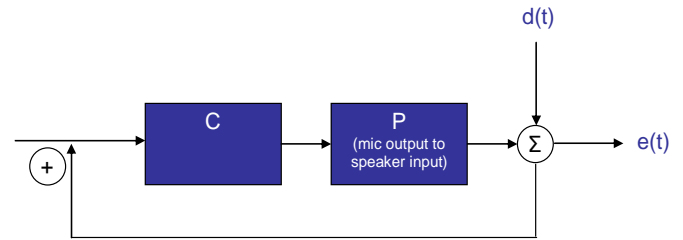


FIGURE 3. A BLOCK DIAGRAM FOR A GENERAL POSITIVE-FEEDBACK CONTROL SCHEME.

The error signal is the result of the superposition of the direct disturbance signal and the modified disturbance signal after it is fed back through $C \cdot P$. In the frequency domain, the error signal can be written as

$$E(j\omega) = D(j\omega) \left[\frac{1}{1 - C(j\omega)P(j\omega)} \right] \quad (1)$$

The error signal is minimized when the magnitude of $C \cdot P$ is maximized at each frequency. This is accomplished by defining the gain, K , of the controller. It is also observed that values of $C \cdot P$ close to unity will result in amplification of the disturbance signal that would result in system instability.

Proper stability margins should be employed when designing feedback controllers. Two common measures of stability are the gain margin (GM) and phase margin (PM) [17]. The gain margin is defined as the factor (in a linear scale) by which the gain can be increased before instability occurs. For a positive feedback control system, the gain margin is defined at the

frequencies where the phase angle crosses 0° and 360° . The magnitude of the frequency response function must be less than unity (on a linear magnitude scale; 0 dB on a log magnitude scale) at these frequencies or instability will result. A Bode plot of a stable fictitious system is shown in Figure 4. The gain margins are represented by G_0 and G_1 .

An alternative stability criterion is the phase margin, which is defined as the phase angle cushion that exists between the phase of C·P and either 0° or 360° when the magnitude of C·P is unity on a linear magnitude scale. The phase margins are represented by ϕ_0 and ϕ_1 in Figure 4. The choice of appropriate gain or phase margins is left up to the designer, but gain margins of 6 dB and phase margins of 30° are usually recommended to allow for dynamic uncertainties in either the plant or the controller [18,19].

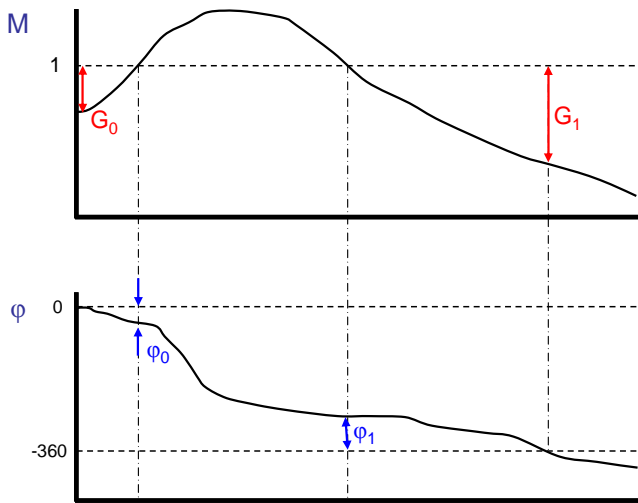


FIGURE 4. MAGNITUDE AND PHASE RESPONSE OF A FICTITIOUS SYSTEM. THE GAIN MARGINS G_0 AND G_1 AND THE PHASE MARGINS ϕ_0 AND ϕ_1 ARE DRAWN.

Frequency response design method

The frequency response design method is often used when the frequency response function of the plant, P, is of sufficiently high order that an accurate analytical model is impractical. In other words, the plant has high frequency dynamics that cannot be accurately modeled but are vital to the control performance. This method involves measuring the frequency response function of the plant and then designing a controller to ensure the desired stability margins are met. This is a practical design approach when hardware can be built and modified at low cost.

Measured frequency response functions

Since the high frequency dynamics of the plant shown in Figure 3 could not be modeled accurately, the frequency response design method was utilized. Broadband noise was

fed into a loudspeaker and the output of the attached accelerometer was measured. The plant transfer function was obtained from these two signals and is shown in Figure 5.

The resonance frequency of the speaker is 70 Hz. The roll-off of the magnitude response below this frequency is due to the loudspeaker's inability to produce sufficient vibration amplitude below its resonance. The peak near 2 kHz is due to an operating shape of the speaker cone that has been shifted down in frequency by mass loading the cone with the accelerometer. The magnitude and phase response is relatively flat between these two prominent spectral features.

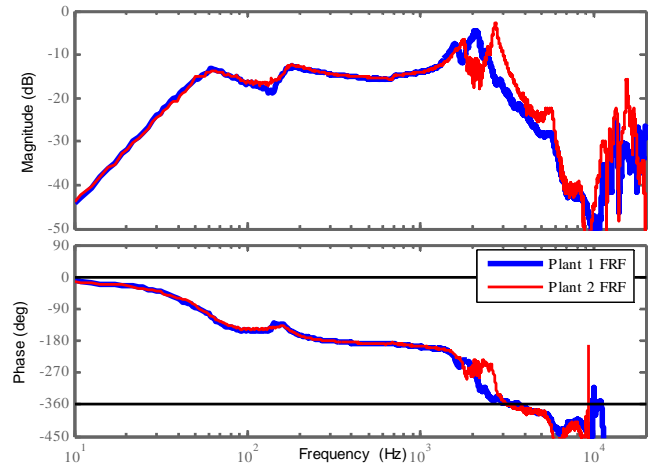


FIGURE 5. MEASURED MAGNITUDE AND PHASE RESPONSE OF EACH DPAP PLANT. THE PHASE STABILITY BOUNDS OF 0° AND 360° ARE DRAWN IN THE PHASE PLOT WITH HORIZONTAL LINES.

Controller design

Analog active noise control has been somewhat abandoned in recent years in favor of digital control regimes. The benefits of analog active noise control are effective control of broadband noise, extremely low signal processing time, inexpensive circuit implementation, and simpler control strategies. An analog feedback controller was designed to minimize the vibration amplitude of each panel. For ease of circuit implementation, it was desired that the transfer function of the control circuit be no more than 2nd order. A low-pass, notch filter was selected and implemented using a Fleischer-Tow biquadratic circuit [20, 21]. The electrical components of each control circuit included three operational amplifiers, eight resistors, and two capacitors. The measured transfer function of the controller in series with each plant is shown in Figure 6.

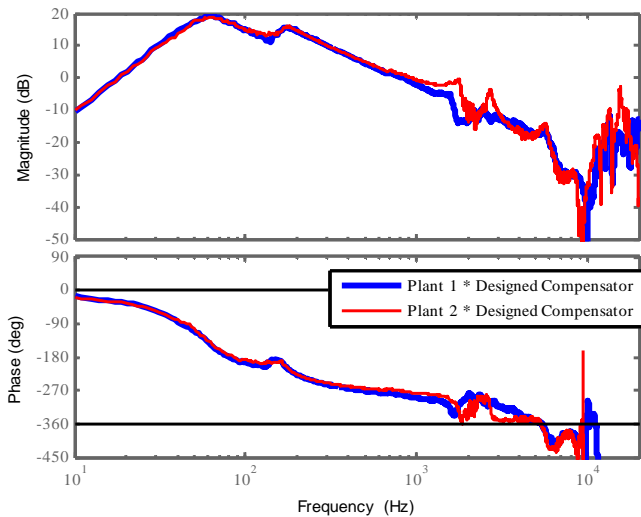


FIGURE 6. MEASURED MAGNITUDE AND PHASE RESPONSE OF AN ANALOG FEEDBACK CONTROLLER IN SERIES WITH EACH DPAP PLANT.

From this figure it is seen that band in which control should be expected lies between 20 Hz and 1 kHz. The magnitude ratio is greater than unity (0 dB) inside this band while the phase is within the stable region of 0-360°. Outside of this band, the magnitude ratio is less than unity (0 dB), so that there will not be unstable amplification of the disturbance signal. Each partition should produce a maximum vibration reduction of 20 dB near 70 Hz with tapering vibration reductions on either side of this peak until the limits of the control band are reached. During the design of the controller, a minimum phase margin of 20° was intended near 1.5 kHz. However, during experimentation, the gain was increased beyond what is depicted in Figure 6 until the instability point near 16 kHz was observed. The gain was then reduced slightly until stability was reestablished. Increasing the gain in this manner shifted the magnitude curve of Figure 6 up by 5 dB and allowed for 25 dB maximum vibration attenuation on each panel.

MEASUREMENT SETUP

Measurement apparatus

A plane wave impedance tube measurement technique was used to determine the normal incidence transmission loss of the DPAP and of a passive single panel partition. The measurement apparatus is depicted in Figure 7. One end of the source side tube was fitted with a loudspeaker which served as the disturbance source. The transmission loss module was inserted in the space between the source side tube and the receiving side tube. The end of the receiving side tube was fitted with a 1.35 m anechoic termination designed to be anechoic to 60 Hz [22]. A two microphone transfer function method of measuring in-duct acoustic properties was implemented [23, 24].

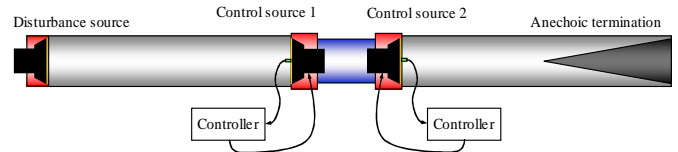


FIGURE 7. A DIAGRAM OF THE MEASUREMENT SETUP, INCLUDING THE DISTURBANCE SOURCE, SOURCE-SIDE AND RECEIVING-SIDE TUBES, THE DPAP MODULE, AND ANECHOIC TERMINATION.

Measurement system qualification

The absorption coefficient, α , of the anechoic termination was measured using the two microphone technique. By strict definition, the anechoic cutoff frequency is the frequency at which α drops below 0.99. The measured absorption coefficient is plotted as a function of frequency in Figure 8. By strict definition, the wedge is anechoic to 195 Hz, but the absorption coefficient is greater than 0.90 all the way to 50 Hz. The lack of a perfectly anechoic termination will result in a small dB error in the transmission loss at low frequencies.

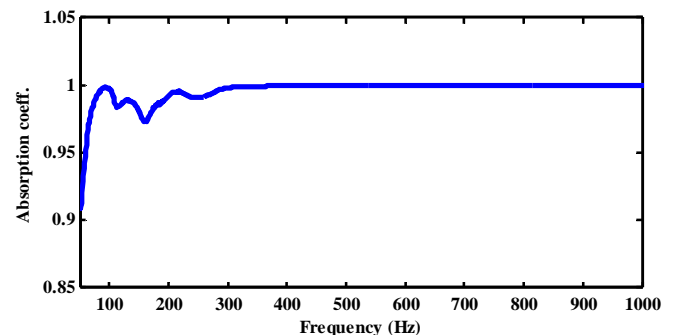


FIGURE 8. MEASURED ABSORPTION COEFFICIENT, α , FOR THE ANECHOIC TERMINATION.

This dB error was calculated to be less than 1.5 dB below 300 Hz and less than 1 dB above. Consequently, the lower measurement limit was 50 Hz. The upper measurement limit was 1.3 kHz and was imposed by the microphone spacing of the two microphone technique. The first cross mode of the duct was 2 kHz; well above the bandwidth of interest. The measurement bandwidth was chosen to be 50-1,000 Hz.

EXPERIMENTAL RESULTS

Error sensor attenuation

The voltage output from each accelerometer was recorded during the transmission loss measurement. The attenuation in these error sensors was calculated as the dB difference in the voltage signal between the active and passive module configurations. Three active DPAP configurations were measured: 1) both panels active, 2) incident panel (panel 1) active, and 3) transmitting panel (panel 2) active. Both the single panel and double panel passive configurations were measured while the speaker terminals had open-circuits. The error sensor attenuations for both panels under each of the three active configurations are shown in Figure 9.

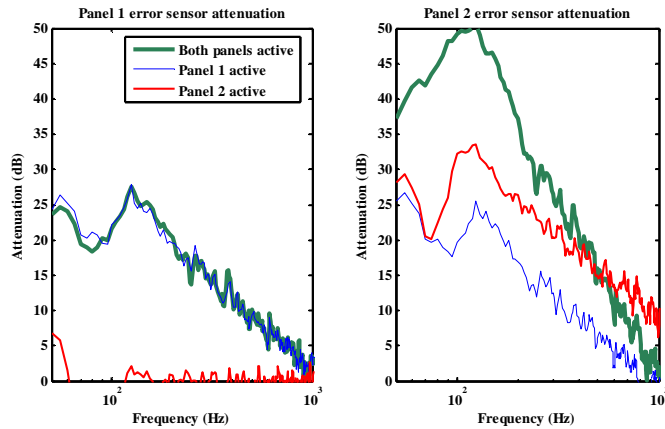


FIGURE 9. ERROR SENSOR ATTENUATIONS FOR EACH PANEL OF THE DPAP MODULE UNDER THREE DIFFERENT ACTIVE CONTROL CONFIGURATIONS.

It was expected that actively controlling the incident panel would reduce the vibration amplitude of both panels. This is confirmed in Figure 9. However, it was observed that actively controlling the transmitting panel had no effect on the vibration amplitude of the incident panel. This result indicates that the acoustic coupling between the two panels is negligible compared to the direct actuation path and that each panel can be controlled independent of the other. As was hypothesized, the error sensor attenuation of panel 2 is significantly larger when both panels are actively controlled.

Scanning laser vibrometer

A scanning laser Doppler vibrometer (SLDV) system was used to measure the surface velocity of the transmitting panel (panel 2). It is possible that the vibration amplitude was reduced at the accelerometer position but increased elsewhere. 358 scan points were defined on the speaker cone and surround. The SLDV was used to see if the reduction at the error sensor was a localized or whether the effect was global. The scan points are displayed in Figure 10.

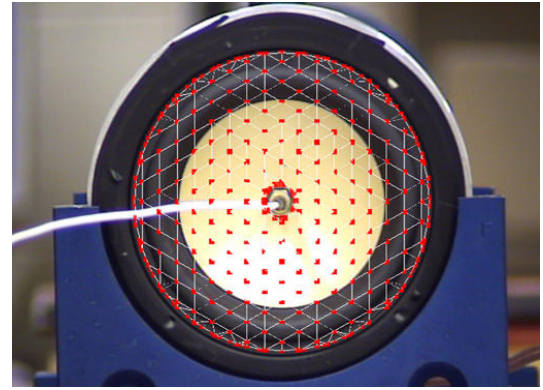


FIGURE 10. SLDV SCAN POINT DISTRIBUTION ON THE CONE AND SURROUND OF THE TRANSMITTING PANEL OF THE DPAP.

The surface velocity at each scan point was measured for the passive and the three active configurations of the double panel module. The RMS surface velocities are displayed in Figure 11 for 112 Hz. The surface velocities are displayed on a dB scale to accentuate the differences between single-panel and double panel control.

Figure 11(a) shows the RMS amplitudes for the passive configuration. The cone velocity is uniform over the area with an amplitude near 50 dB (0 dB = 100 $\mu\text{m/s}$).

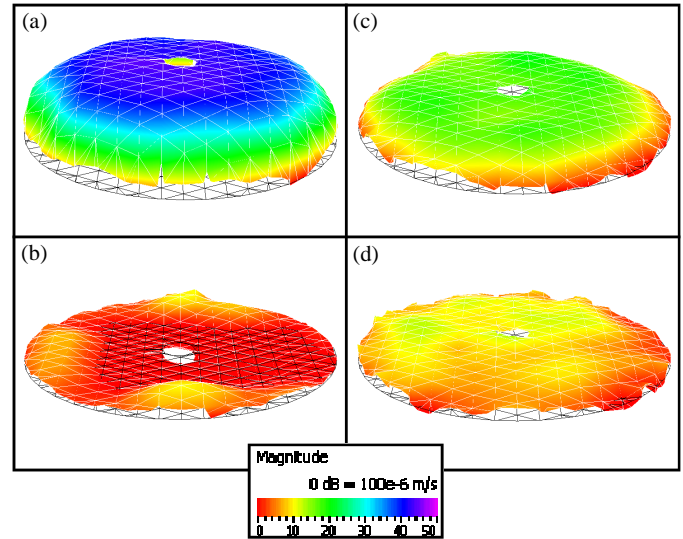


FIGURE 11. RMS SURFACE VELOCITIES ON THE TRANSMITTING PANEL FOR THREE ACTIVE AND ONE PASSIVE DPAP CONTROL CONFIGURATIONS: (A) PASSIVE, (B) BOTH PANELS ACTIVELY CONTROLLED, (C) INCIDENT PANEL ACTIVELY CONTROLLED, (D) TRANSMITTING PANEL ACTIVELY CONTROLLED (NOTE 0 DB = 100 $\mu\text{m/s}$).

Figure 11(c) shows the effect of controlling the incident panel (panel 1) on the velocity amplitude of the transmitting panel (panel 2). It is observed that there is residual vibration on the transmitting panel on the order of 15 dB. Figure 11(d) shows that controlling the transmitting panel directly results in better vibration amplitude reduction than controlling the incident panel. However, the residual vibration in this case is still on the order of 10 dB. Most importantly, these scans show that the reduction in vibration amplitude occurs everywhere on the transmitting surface and that the error signal attenuation is not just a localized effect.

Transmission loss results

The normal-incidence sound transmission loss was measured using the two microphone impedance tube technique. The transmission loss was measured for two passive and three active configurations. The results are shown in Figure 12.

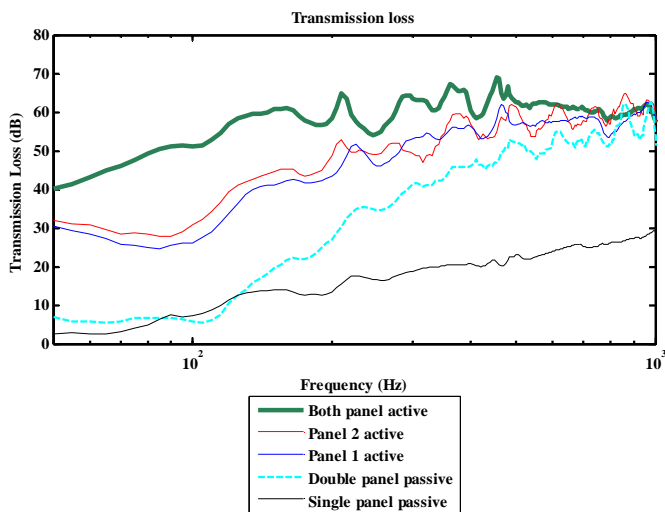


FIGURE 12. NORMAL-INCIDENCE TRANSMISSION LOSS MEASUREMENT FOR TWO PASSIVE AND THREE ACTIVE CONFIGURATIONS.

The passive transmission loss of the both the single and double panel partitions are poor at low frequencies. This is due to the resonance effects of each panel, as well as the mass-air-mass resonance between the panels. In the case of the passive double panel partition, at frequencies above the mass-air-mass resonance, the transmission loss rises at the expected rate of 18 dB/octave [25]. The transmission loss improves considerably when a single panel of the DPAP is controlled, with direct control of the transmitting panel slightly outperforming direct control of the incident panel. This result agrees with the results of the error sensor attenuation and SLDV measurements. The best transmission loss performance is produced by simultaneous, direct actuation of each panel of the DPAP. The TL performance of the DPAP is nearly doubled at 100 Hz; going from 25 dB for single panel control to 50 dB for double panel control.

It should also be noted that the actively controlled module gracefully transitions into passive control at the upper limit of the control bandwidth, effectively becoming a hybrid passive/active system near 1 kHz.

The average transmission loss over the measurement bandwidth (50-1,000 Hz) was computed for the two passive and three active configurations. The average results are listed in Table 1.

TABLE 1. AVERAGE TRANSMISSION LOSS FOR TWO PASSIVE AND THREE ACTIVE CONTROL CONFIGURATIONS. THE TRANSMISSION LOSS WAS AVERAGED OVER THE MEASUREMENT BANDWIDTH OF 50-1,000 HZ.

	TL Avg (50-1,000 Hz)
SP Passive	21
DP passive	44
DP Incident panel active	53
DP Transmitting panel active	54
DP Both panels active	60

The DPAP outperformed the passive single panel by 39 dB and the passive double panel by 16 dB when both panels were controlled. However, the double panel passive partition had significant transmission loss above 500 Hz so the average of 16 dB is not representative of the tremendous increase in low frequency control. The dual-controlled DPAP outperformed the passive double panel partition by an average of 27 dB over the bandwidth of 50-500 Hz.

SUMMARY AND CONCLUSIONS

Hardware design of an actively controlled double panel partition was introduced. Design choices included two directly actuated panels (via speakers), module symmetry, collocated sensor/actuator pairs, and an analog feedback controller. The purpose of each design decision was explained.

The frequency response method of controller design was used to create a 2nd order Fleischer-Tow biquad control circuit. This circuit was implemented using operational amplifiers, resistors, and capacitors. A phase margin of 20° was observed in the design.

A measurement setup was created in which normal-incidence transmission loss measurements were conducted. The anechoic termination was qualified and limits of measurement error were determined to be less than 1.5 dB at all frequencies. The measurement bandwidth for the system was 50 Hz – 1 kHz.

Experimental results showed that simultaneous actuation of both panels of the DPAP resulted in better error sensor attenuation than control of a single panel. SLDV measurements showed that this reduction in the vibration amplitude was global over the entire transmitting surface. The same performance was observed in the transmission loss measurement.

The dual-controlled DPAP outperformed the single panel passive control by 39 dB over the measurement bandwidth (50-1,000 Hz). Additionally, the DPAP outperformed the passive double panel partition by 16 dB over the same bandwidth and by 27 dB over the bandwidth of 50-500 Hz.

The research has produced a module that is also bidirectional—meaning that it can block sound transmission in either direction through the device. It also has shown that simultaneous, independent/decoupled/SISO analog feedback control on both panels is an effective active control strategy. Future work would include the extension of the small experimental module to a module with a larger cross section, experimentation with this module design in an active segmented partition (ASP), development of lightweight and low cost actuators, measurement of transmission loss when sound is incident on both panels at the same time, and random incidence transmission loss measurements.

REFERENCES

- [1] Fuller, C. R., 1991, “Active control of sound radiation from a vibrating rectangular panel by sound sources and vibration inputs: An experimental comparison,” *Journal of Sound and Vibration* **145**, pp. 195-215.
- [2] Fuller, C. R., Silcox, R. J., 1992, “Active structural acoustic control,” *Journal of the Acoustical Society of America* **91**, pp. 519.
- [3] Thomas, D. R., Nelson, P. A., Elliott, S. J., Pinnington, R. J., 1993, “An experimental investigation into the active control of sound transmission through stiff light composite panels,” *Noise Control Engineering Journal* **41**, pp. 273-279.
- [4] Johnson, M. E., Elliott, S. J., 1995, “Active control of sound radiation using volume velocity cancellation,” *Journal of the Acoustical Society of America* **98**, pp. 2174-2186.
- [5] St. Pierre, R. L., Koopmann, G. H., Chen, W., 1997, “Volume velocity control of sound transmission through composite panels,” *Journal of Sound and Vibration* **210**, pp. 441-460.
- [6] Hirsch, S. M., Sun, J.Q., Jolley, M.R., 2000, “An analytical study of interior noise control using segmented panels,” *Journal of Sound and Vibration* **231**, pp. 1007-1021.
- [7] Hirsch, S. M., Meyer, N.E., Westervelt, M.A., King, P., Li, F. J., Petrova, M. V., Sun, J.Q., 2000, “Experimental study of smart segmented trim panels for aircraft interior noise control,” *Journal of Sound and Vibration* **231**, pp. 1023-1037.
- [8] Bingham, B., Atalla, M. J., Hagood, N. W., 2001, “Comparison of structural-acoustic control designs on an active composite panel,” *Journal of Sound and Vibration* **244**, pp. 761-778.
- [9] Petitjean, B., Legrain, I., 2002, “Active control experiments for acoustic radiation reduction of a sandwich panel: Feedback and feedforward investigations,” *Journal of Sound and Vibration* **252**, pp. 19-36.
- [10] Gardonio, P., Bianchi, E., Elliott, S.J., 2004, “Smart panel with multiple decentralized units for the control of sound transmission. Part I: theoretical predictions,” *Journal of Sound and Vibration* **274**, pp. 163-192.
- [11] Gardonio, P., Bianchi, E., Elliott, S.J., 2004, “Smart panel with multiple decentralized units for the control of sound transmission. Part II: design of the decentralized control units,” *Journal of Sound and Vibration* **274**, pp. 193-213.
- [12] Gardonio, P., Bianchi, E., Elliott, S.J., 2004, “Smart panel with multiple decentralized units for the control of sound transmission. Part III: control system implementation,” *Journal of Sound and Vibration* **274**, pp. 215-232.
- [13] Leishman, T. W., 2000, “Active control of sound transmission through partitions composed of discretely controlled modules,” Ph.D. thesis, The Pennsylvania State University, University Park, PA.
- [14] Leishman, T. W., Tichy, J., 2005, “A theoretical and numerical analysis of vibration-controlled modules for use in active segmented partitions,” *Journal of the Acoustical Society of America* **118**, pp. 1424-1438.
- [15] Leishman, T. W., Tichy, J., 2005, “An experimental investigation of two module configurations for use in active segmented partitions,” *Journal of the Acoustical Society of America* **118**, pp. 1439-1451.
- [16] Leishman, T. W., Tichy, J., 2005, “An experimental investigation of two active segmented partition arrays,” *Journal of the Acoustical Society of America* **118**, pp. 3050-3063.
- [17] Franklin, G. F., Powell, J. D., Emami-Naeini, A., 2006, *Feedback Control of Dynamic Systems, 5th Ed*, Pearson Prentice Hall, New Jersey.
- [18] Nelson, P. A., Elliott, S. J., 1992, *Active Control of Sound* Academic, London.
- [19] Yu, S. H., Hu, J. S., “Controller design for active noise cancellation headphones using experimental raw data,” *IEEE/ASME Transactions on Mechatronics*, **6**, pp. 483-490 (2001).
- [20] Fleischer, P.E., Tow, J., 1973, “Design formulas for biquad active filters using three operational amplifiers,” *Proceedings of the IEEE*, pp. 662-663.
- [21] Su, K., 2002, *Analog Filters, 2nd Edition*, Kluwer Academic, MA.
- [22] Beranek, L. L., Sleeper, H. P. Jr., 1946, “The design and construction of anechoic sound chambers,” *Journal of the Acoustical Society of America* **18**, pp. 140-150.
- [23] Chung, J.Y., Blaser, D. A., 1980, “Transfer function method of measuring in-duct acoustic properties. I.

Theory,” *Journal of the Acoustical Society of America* **68**, pp. 907-913.

[24] Chung, J. Y., Blaser, D. A., 1980, “Transfer function method of measuring in-duct acoustic properties. II. Experiment,” *Journal of the Acoustical Society of America* **68**, pp. 914-921.

[25] Fahy, F. J., 2001, *Sound and Structural Vibration, Radiation, Transmission, and Response*, Academic, London.